ANNULAR HONEYCOMB SEALS: TEST RESULTS FOR LEAKAGE AND ROTORDYNAMIC COEFFICIENTS; COMPARISONS TO LABYRINTH AND SMOOTH CONFIGURATIONS[1]

Dara Childs, David Elrod, and Keith Hale
Texas A&M University
College Station, Texas 77843, U.S.A.

Test results are presented for leakage and rotordynamic coefficients for seven honeycomb seals. All seals have the same radius, length, and clearance; however, the cell depths and diameters are varied. Rotordynamic data, which are presented, consist of the direct and cross-coupled stiffness coefficients and the direct damping coefficients. The rotordynamic-coefficient data show a considerable sensitivity to changes in cell dimensions; however, no clear trends are identifiable.

Comparisons of test data for the honeycomb seals with labyrinth and smooth annular seals show the honeycomb seal had the best sealing (minimum leakage) performance, followed in order by the labyrinth and smooth seals. For prerotated fluid entering the seal, in the direction of shaft rotation, the honeycomb seal has the best rotordynamic stability followed in order by the labyrinth and smooth. For no prerotation, or fluid prerotation against shaft rotation, the labyrinth seal has the best rotordynamic stability followed in order by the smooth and honeycomb seals.

[1]This work was supported in part by NASA Grant NAG3-181 from NASA Lewis Research Center (Technical Monitor, Robert Hendricks) and AFOSR Contract F49620-82-K-0033 (Technical Monitor, Tony Amos)

NOMENCLATURE

C, c	Direct and cross-coupled damping coefficients (FT/L)
$\overline{C}, \overline{c}$	Normalized direct and cross-coupled damping coefficients (T), defined in Eq. (3)
Cr	Radial clearance (L)
D	Diameter (L)
F	Seal reaction-force magnitude (F)
$f = k/C\omega$	Whirl frequency ratio (dimensionless)
K, k	Direct and cross-coupled stiffness coefficients (F/L)
$\overline{K}, \overline{k}$	Dimensionless direct and cross-coupled stiffness coefficients, defined in Eq. (3)
L	Seal length (L)
P	Fluid pressure (F/L^2)
R	Seal radius (L)
R_c	Gas constant for air
T	Fluid temperature (K)
$U_{\theta o}$	Seal inlet tangential velocity (L/T)
$u_{\theta o} = U_{\theta o}/R\omega$	Nondimensionalized seal inlet tangential velocity
X, Y	Rotor to stator relative displacement components (L)
Φ	Flow coefficient, defined in Eq. (4)
ω	Shaft angular velocity $(1/T)$

Subscripts

b	Sump value (dimensionless)
r	Reservoir value, radial component

Introduction

Annular seals using honeycomb stators and smooth rotors are occasionally used in turbomachinery, although not as commonly as labyrinths. This type of seal is illustrated in figure 1.

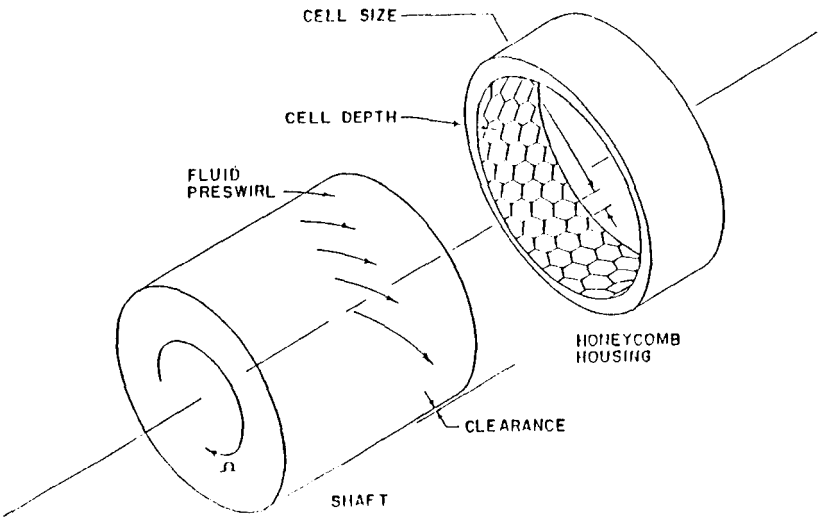

Figure 1. Honeycomb seal geometry.

The model used to define the reaction-force/motion relationship for a centered gas seal is

$$-\begin{Bmatrix} F_X \\ F_Y \end{Bmatrix} = \begin{bmatrix} K & k \\ -k & K \end{bmatrix} \begin{Bmatrix} X \\ Y \end{Bmatrix} + \begin{bmatrix} C & c \\ -c & C \end{bmatrix} \begin{Bmatrix} \dot{X} \\ \dot{Y} \end{Bmatrix}. \tag{1}$$

The test apparatus used here can separately measure the four coefficients of Eq. (1); however, the magnitude of the cross-coupled damping coefficient c is comparable to our measurement uncertainty, and is accordingly not presented. Fortunately this coefficient has a minor influence on compressor and turbine rotordynamics. Data are presented for the direct stiffness K, although (for gas seals) this coefficient also does not have a major influence on rotordynamics. The cross-coupled stiffness k and direct damping C coefficients are of primary influence with respect to rotordynamic stability, since k and C oppose each other in trying to destabilize/stabilize a rotor.

The whirl frequency ratio

$$f = \frac{k}{C\omega} \tag{2}$$

is a useful nondimensional parameter for comparing the stability properties of seals. For circular synchronous orbits, it provides a ratio between the destabilizing force component due to k and the stabilizing force component due to C.

To the authors' knowledge, Benckert and Wachter (1980) have presented the only prior test data for honeycomb seals. Their test rig could only measure stiffness coefficients. Their data, for a single honeycomb configuration, showed large values for k as compared to results for labyrinth seals. Experience with the SSME (Space Shuttle Main Engine) HPOTP (High Pressure Oxygen Turbopump) provides contrary evidence which suggests that honeycomb

seals are more stable than labyrinth seals; viz., replacement of a labyrinth turbine interstage seal with a honeycomb configuration eliminated a rotordynamic instability problem and reduced synchronous vibration levels. The data presented here were stimulated by the SSME experience and is the first presentation of damping data for honeycomb seals and the first systematic presentation of rotordynamic data for a range of honeycomb - cell dimensions.

TEST APPARATUS AND APPROACH

The contents of this section review the test apparatus, test variables, and nondimensionalization of these results before presenting leakage and rotordynamic data.

Test Apparatus

A complete description of the test apparatus is provided by Childs et al. (1986). As illustrated in figure 2, the rotor shaft is suspended, pendulum fashion, from an upper, rigidly-mounted, pivot shaft. This arrangement allows horizontal (harmonic) motion of the rotor. A cam within the pivot shaft provides vertical (static) positioning of the rotor. The rotor is excited, horizontally, by a hydraulic-shaker head which acts on the rotor-shaft housing. The design of the test rig, which is further illustrated in figure 3, permits the installation of various rotor/stator combinations. The test apparatus has been modified since the 1986 reference to permit an increase in top operating speeds from 8,000 to 16,000 *cpm*. Changes include the use of a hydraulically fitted rotor, the introduction of high-speed carbon seals, and the replacement of a roller-element thrust bearing with a Torrington, water-lubricated, swing-pad bearing. The stator of figure 3 is supported in the test section housing by three piezo-electric, quartz, load cells in a trihedral configuration. These load cells measure the pressure-induced forces due to rotor motion within the stator. Accelerometers are provided on the stator to correct for acceleration-induced forces which are measured by the load cell.

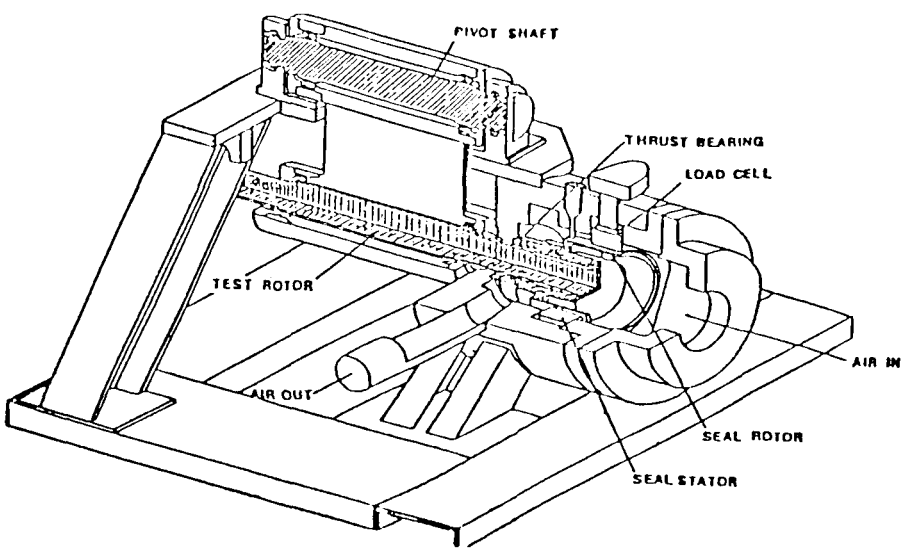

Figure 2. Test Apparatus.

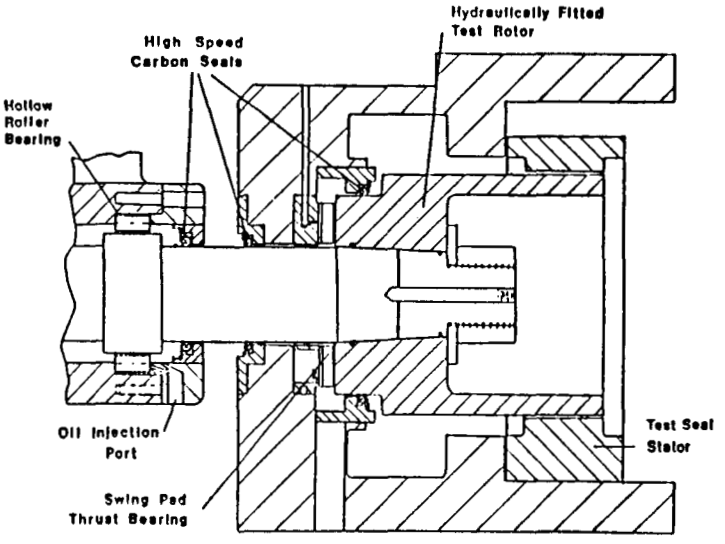

Figure 3. Test-section cross section.

Honeycomb-Seal Dimensions

Table 1 Contains dimensions for the honeycomb seals. The cell sizes cover the normal range for gas-turbine and compressor applications. The 0.74 *mm* cell depths tend to be smaller than common practice because of earlier experience with liquid seals, Childs and Kim (1985); however, the depths, 1.47 and 1.91 *mm*, are comparable to industrial practice.

Table 1. Honeycomb Seal Dimensions;
$L = 50.8mm, C_r = 0.41mm, R = 151.36mm.$

Seal	Cell Size	Cell Depth
1	0.51 mm	0.74 mm
2	0.51 mm	1.47 mm
3	0.79 mm	0.74 mm
4	0.79 mm	1.47 mm
5	1.57 mm	0.74 mm
6	1.57 mm	1.47 mm
7	1.57 mm	1.91 mm

Test Variables

When shaking about the centered position, the dynamic-seal-apparatus is capable of controlling the following four independent variables: *pressure ratio, rotor speed, shake frequency, and inlet circumferential velocity.* The actual test points for three of these variables are shown in table 2.

Table 2. Test Variables

Pressure Ratio	Rotor Speeds	Inlet Circumferential Velocities
1 - 3.03	1 - 3000 cpm	−2 - High velocity against rotation
2 - 4.45	2 - 6000 cpm	−1 - Low velocity against rotation
3 - 5.70	3 - 9500 cpm	0 - Zero circumferential velocity
4 - 6.95	4 - 13000 cpm	1 - Low velocity with rotation
5 - 8.00	5 - 16000 cpm	2 - High velocity with rotation

The inlet circumferential velocities are controlled using the inlet guide vanes shown in figure 4. The guide vanes are contained in sleeves and located immediately upstream of the test seal. The no-prerotation case is obtained without guide vanes. "High" and "low" prerotation velocities are obtained for the different, guide-vane-depths "A" of figure 4. The inlet circumferential velocity is calculated from measured values for the volumetric flow rate, upstream temperature and pressure, and a flow-turning correction in accordance with Cohen et al. (1972). The circumferential velocity can not be varied arbitrarily, because it depends on the supply pressure and the flow resistance of the seal being tested.

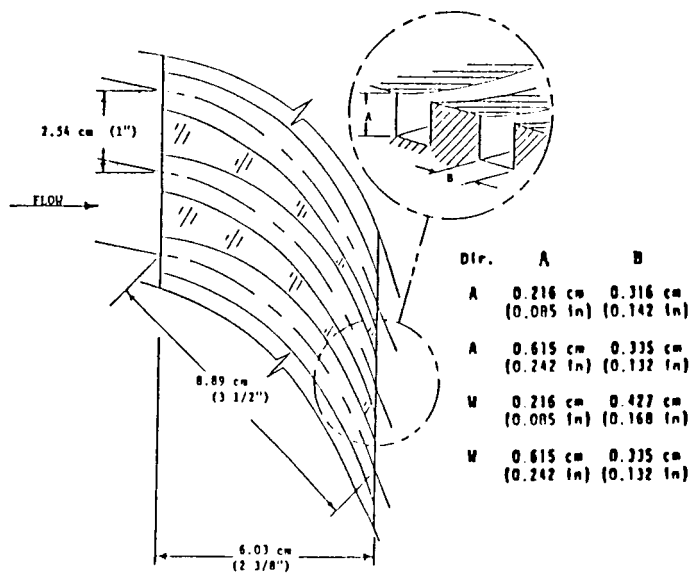

Figure 4. Inlet-guide-vane detail.

Figure 5 illustrates the inlet circumferential velocity versus pressure ratio for the five vane settings. The results are for 3,000 *cpm* and show $U_{\theta o}$ to be insensitive to changes in the pressure ratio for a given vane setting. Although not illustrated, the velocity tends to decrease with rotor speed, mainly because the rotor grows with increasing speed and reduces the leakage. The ratio of inlet circumferential velocity to rotor surface velocity, $u_{\theta o}$, ranged from about −3.1 to about 3.8. Although the larger numbers are unrealistic, they give insight into the effects of inlet circumferential velocity that would otherwise go unnoticed. The insensitivity of $U_{\theta o}$ to changes in pressure ratio illustrated in figure 5 are typical for all annular gas seals which have been tested.

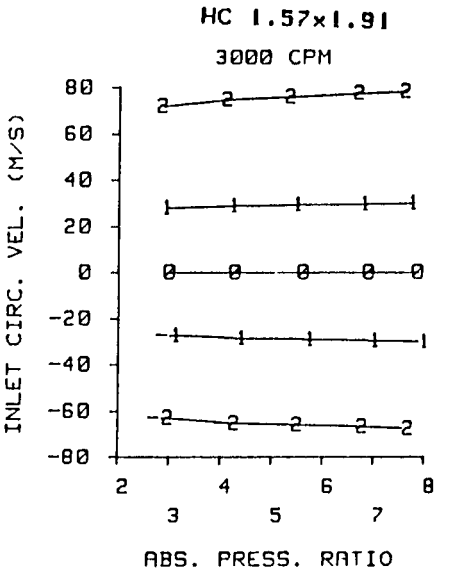

Figure 5. Inlet-circumferential velocity versus pressure ratio for seal 7 of table 1.

HONEYCOMB SEAL ROTORDYNAMIC COEFFICIENT RESULTS

Relative Uncertainty

The uncertainty in the dynamic coefficients can be determined using the method described by Holman (1978). The uncertainty in the force, excitation frequency, and displacement measurements are 0.44 N (0.1 lb), 0.065 Hz, and 0.0013 mm (0.05 mils), respectively. Before normalization, the maximum calculated uncertainty in the stiffness and damping coefficients is 24.1 N/mm (138 lb/in), and 0.072 N-s/mm (0.41 lb-s/in), respectively.

Frequency Dependency of Rotordynamic Coefficients

The stiffness coefficients of the honeycomb seals are shake-frequency-dependent. Previously, frequency-dependent results have been observed for an interlock seal, Childs et al. (1987). However, this characteristic has not been evident in tests of smooth (constant-clearance or taper-geometry) seals, labyrinth-rotor/smooth-stator seals, or labyrinth-rotor-seals. Figures 6 and 7 illustrate K for seals 1 and 7 for the three test frequencies; 38.7, 56.8, and 74.6 Hz. Seals 1 and 7 represent extremes of frequency dependency. Seal 1 is one of the stiffest seals and displays little or no frequency dependency, while seal 7 has low stiffness values and considerable frequency dependency. The results for seal 7 are repeatable and the frequency dependency exceeds the relative uncertainty.

Although not illustrated, the effect on k of changing the shake frequency is greatest for seals 5 and 7, which have the lowest cross-coupled stiffnesses. Changing the shake frequency has little effect on the cross-coupled stiffness of the other five honeycomb seals. The direct damping C is independent of shake frequency.

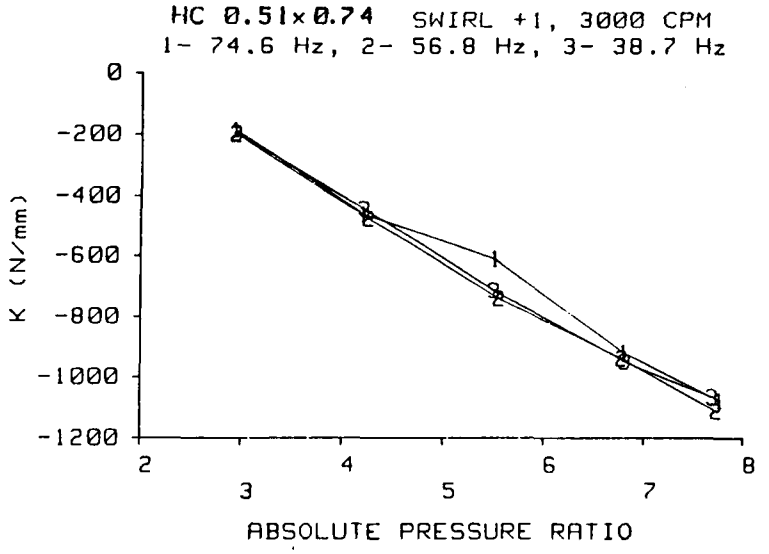

Figure 6. K versus pressure ratio for three excitation frequencies of seal 1 of table 1.

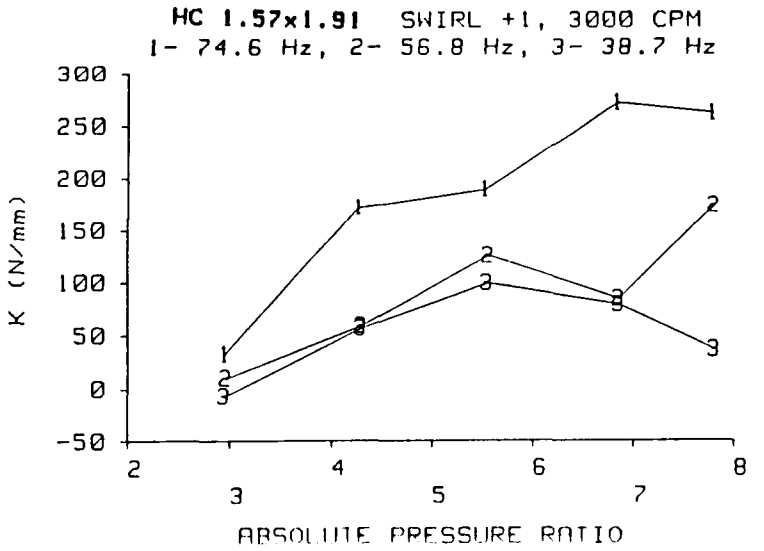

Figure 7. K versus pressure ratio for three excitation frequencies of seal 7 of table 1.

Normalization of Coefficients

Due to thermal and mechanical stresses, the seal rotor grows with changes in the shaft speed. To account for the resulting changes in the radial clearance, the growth was measured over the range of speeds tested. To remove the effect of clearance change, the coefficients are normalized in the following manner:

$$\overline{K} = \frac{KCr}{LD(P_r - P_b)} \qquad \overline{C} = \frac{CCr}{LD(P_r - P_b)}$$
$$\overline{k} = \frac{kCr}{LD(P_r - P_b)} \qquad \overline{c} = \frac{cCr}{LD(P_r - P_b)} \tag{3}$$

Cross-Coupled Stiffness Results

Figure 8 illustrates $\overline{k}$ versus $u_{\theta o}$ at the highest inlet pressure and running speed of table 1 for the seven seals of table 1. Although not illustrated, similar results were obtained at the lowest pressure and highest speed. The figure shows that $\overline{k}$ is positive, i.e., destabilizing, even for negative $u_{\theta o}$. The figure also shows that destabilizing forces are highest for seal 1 and lowest for seal 7. For the two smaller cell sizes, $\overline{k}$ decreases with increasing cell depth. For the largest cell size, $\overline{k}$ increases and then decreases with increasing cell depth. For seals 2, 4, 5, 6, and 7 of table 1, there is little dependence of $\overline{k}$ on $u_{\theta o}$.

Figure 9 shows $\overline{k}$ versus ω for the high inlet pressure of table 2 with $u_{\theta o} = 0$. Similar results are obtained at the lowest pressure. Seal 7 has the best (smallest) $\overline{k}$ of all the seals tested. There is no obvious pattern between changes in $\overline{k}$ and changes in the cell honeycomb dimensions, although the deepest cell depth (seal 7) yields a minimum $\overline{k}$.

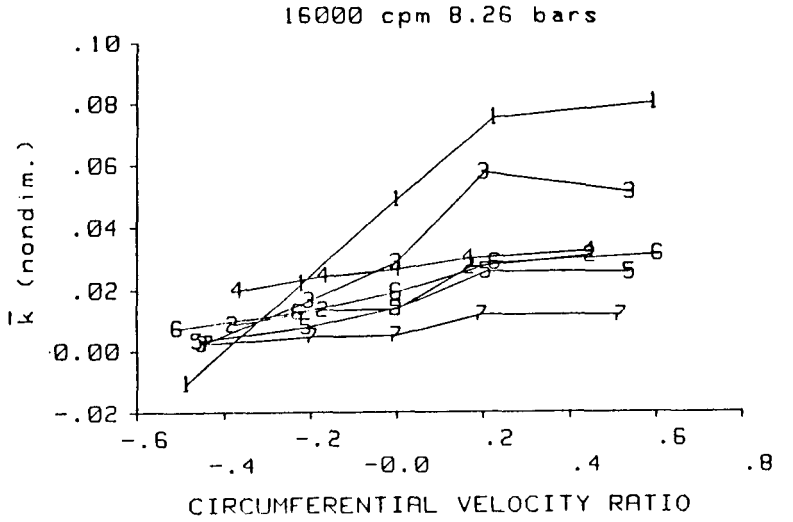

Figure 8. $\overline{k}$ versus $u_{\theta o}$ for the seven honeycomb seals of table 1.

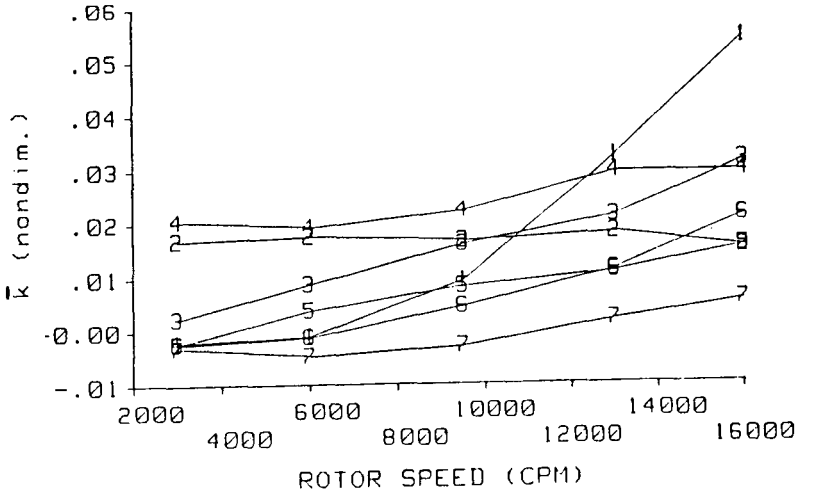

Figure 9. $\overline{k}$ versus ω for the seven honeycomb seals of table 1.

Direct Damping Results

Figure 10 shows $\overline{C}$ versus $u_{\theta o}$ for the lowest and highest inlet pressures and highest rotor speed of table 2. Seals 1 and 3 of table 1 have the highest values of $\overline{C}$. Figure 11 shows that the normalized damping of honeycomb seals 1 and 3 increases with increasing rotor speed. There is no clear trend with increasing ω for the remainder of the honeycomb seals. The highest (best) damping values are generally obtained for seals 1,3, and 4. The worst damping performance is provided by seals 6 and 7 which have the largest cell sizes and depth.

Whirl Frequency Ratio Results

Figure 12 provides comparisons of the whirl frequency ratio f for the seven honeycomb seals at the highest inlet pressure and rotor speed. For the two smaller cell sizes, an increase in cell depth results in a more stable seal (lower f). Seal 5, however, with large shallow cells, is more stable than seal 6. Only seal 1 is less stable than seal 6. Seal 7, with 0.44 mm deeper cells than seal 6, is the most stable seal tested. Obviously, for the larger cell size, f can be quite sensitive to cell depth changes.

Direct Stiffness Results

Figure 13 shows $\overline{K}$ versus $u_{\theta o}$ for the seven honeycomb seals at the highest inlet pressure and rotor speed. $\overline{K}$ is generally negative for seals 1 and 3 and positive for seals 2, 5, 6, and 7. $\overline{K}$ is highest for seal 6, and generally lowest for seal 1. Figure 14 illustrates $\overline{K}$ versus rotor speed for no prerotation of the inlet air. Except for seals 1 and 3, $\overline{K}$ increases as ω increases at both the lowest and highest inlet pressures. About the same results are obtained for the lowest pressure.

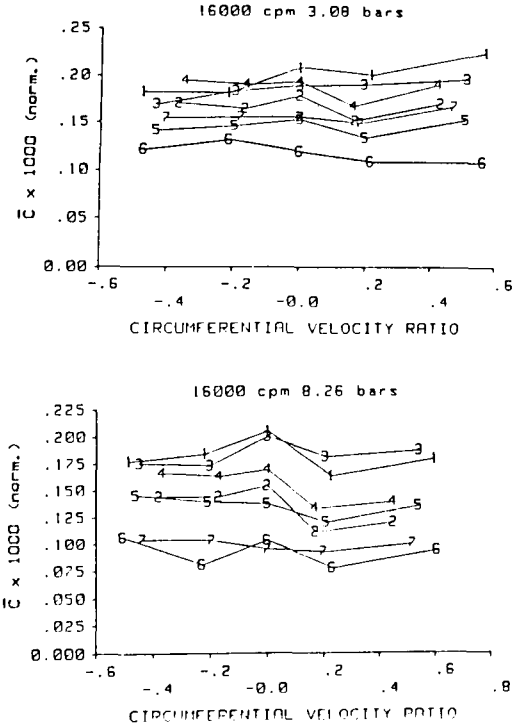

Figure 10. $\overline{C}$ versus $u_{\theta o}$ for the seven honeycomb seals of table 1.

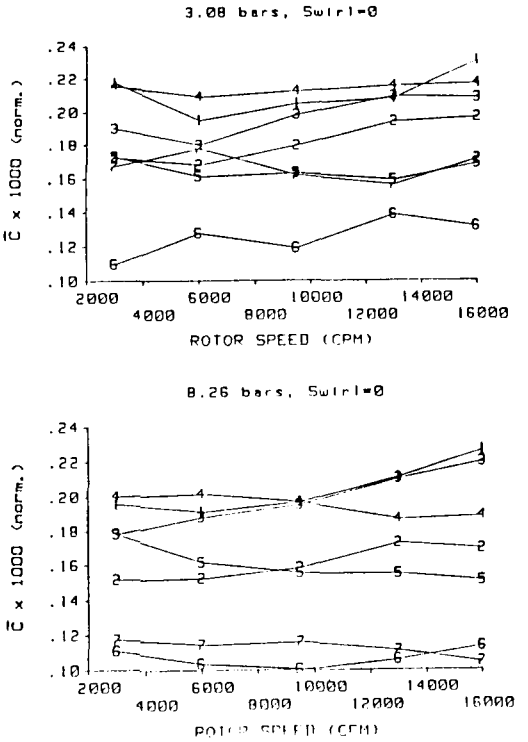

Figure 11. $\overline{C}$ versus ω for the seven honeycomb seals of table 1.

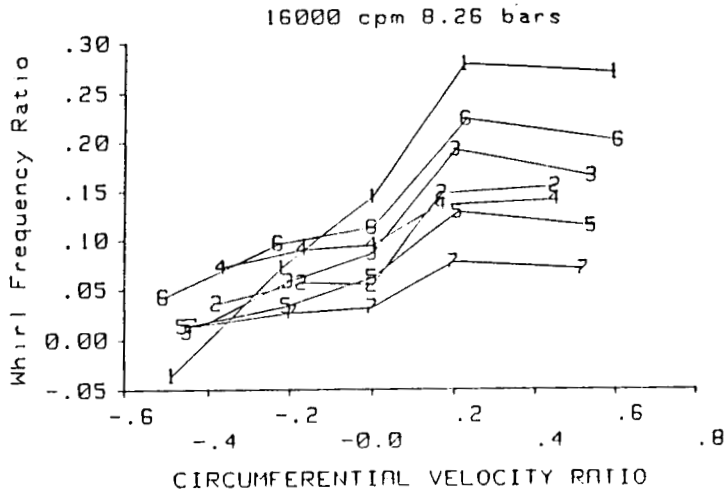

Figure 12. Whirl frequency ratio versus u_{θ_o} for the seven honeycomb seals of table 3.

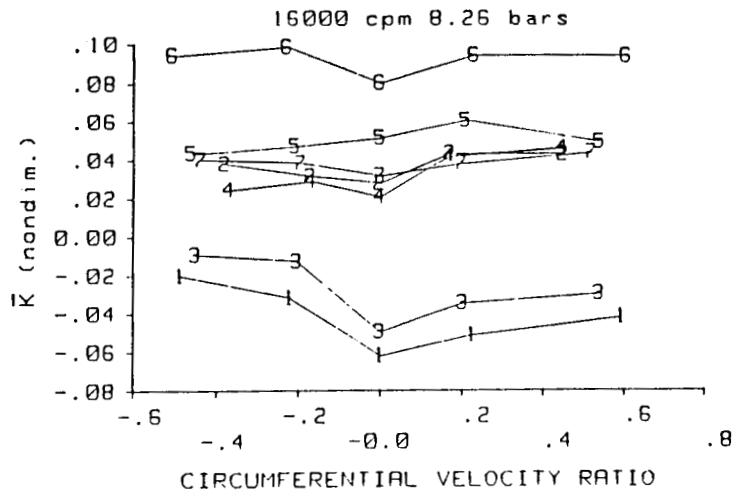

Figure 13. $\overline{K}$ versus u_{θ_o} for the seven honeycomb seals of table 1.

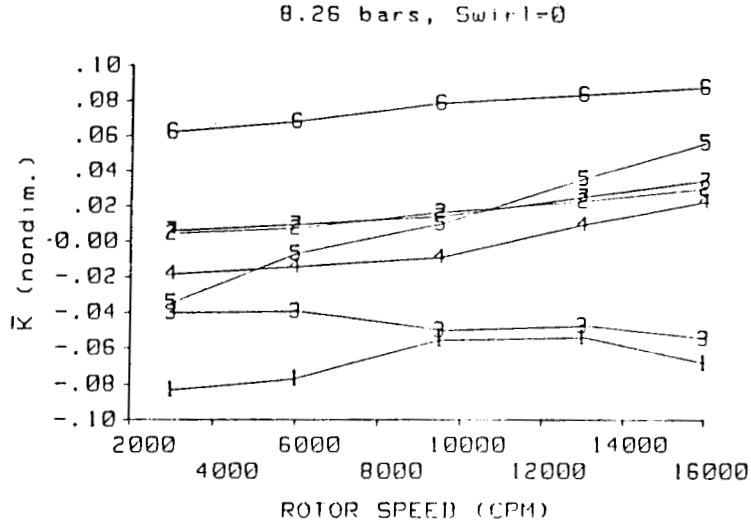

Figure 14. $\overline{K}$ versus ω for the seven honeycomb seals of table 3.

ROTORDYNAMIC COEFFICIENTS: COMPARISONS BETWEEN HONEYCOMB, LABYRINTH, AND SMOOTH SEALS

Comparisons are made in this section for the rotordynamic coefficients of the following seal stators:

(a) honeycomb seal 7 of table 1,
(b) the labyrinth stator of figure 15, and
(c) a smooth stator.

Seal 7 is the most stable honeycomb seal tested, based on a minimum whirl frequency ratio. All seals have the same length (50.8 *mm*), radial clearance (0.41 *mm*) and rotor diameter (151.36 *mm*). The comparative rotordynamic stability of the three seals is of interest in this section. In the following figures, smooth, labyrinth, and honeycomb seal data are labeled S, L, and H, respectively.

Rotordynamic Coefficients

Cross-Coupled Stiffness Results

Figure 16 shows $\overline{k}$ versus $u_{\theta o}$ at the lowest and highest inlet pressure rotor speed of table 2. For the smooth and labyrinth seals (curves S and L, respectively), $\overline{k}$ is negative, i.e. stabilizing, for negative $u_{\theta o}$. For the labyrinth seal, $\overline{k}$ is even stabilizing for no prerotation of the inlet air. For the honeycomb seal, $\overline{k}$ is positive (destabilizing) for all inlet circumferential velocities. For positive $u_{\theta o}$, $\overline{k}$ is almost equally destabilizing for the labyrinth and honeycomb seals. A comparison of figures 8 and 16 reveals that, for positive $u_{\theta o}$, $\overline{k}$ is larger for most of the honeycomb seals than the labyrinth seal as reported earlier by Benckert and Wachter (1980). Although not illustrated, the results of figure 16 also hold for other test pressure conditions.

Figure 17 shows $\overline{k}$ versus ω for the three seals. The results shown are from tests with no prerotation of the inlet air and an inlet pressure of 3.08 bars. For the smooth and honeycomb seals, $\overline{k}$ increases as the rotor speed increases. For the labyrinth seal, $\overline{k}$ is increasingly negative as the rotor speed increases. Childs and Scharrer (1987) have previously noted this type of results for labyrinth seals, as did Hisa et al. (1986). One would expect $\overline{k}$ to eventually begin increasing as ω increases.

Direct Damping Results

Figure 18 shows $\overline{C}$ versus $u_{\theta o}$ for the smooth, labyrinth, and honeycomb seals. $\overline{C}$ for the honeycomb seal is five or six times $\overline{C}$ for the labyrinth seal. At an inlet pressure of 3.08 bars, the smooth and honeycomb seals have about the same normalized direct damping. At 8.26 bars, $\overline{C}$ for the smooth seal is about one-half of $\overline{C}$ for the honeycomb seal when $u_{\theta o}$ is positive. For non-positive $u_{\theta o}$, $\overline{C}$ for the smooth seal is greater than $\overline{C}$ for the honeycomb seal. Note by comparison to figure 10, that most of the other honeycomb seals have substantially higher damping values than seal 7.

Figure 19 shows $\overline{C}$ versus ω for no prerotation of the inlet air and 3.08 bars inlet pressure. In this figure, $\overline{C}$ for the smooth seal increases with increasing rotor speed. For the labyrinth and honeycomb seals, there is little change in $\overline{C}$ with increasing ω.

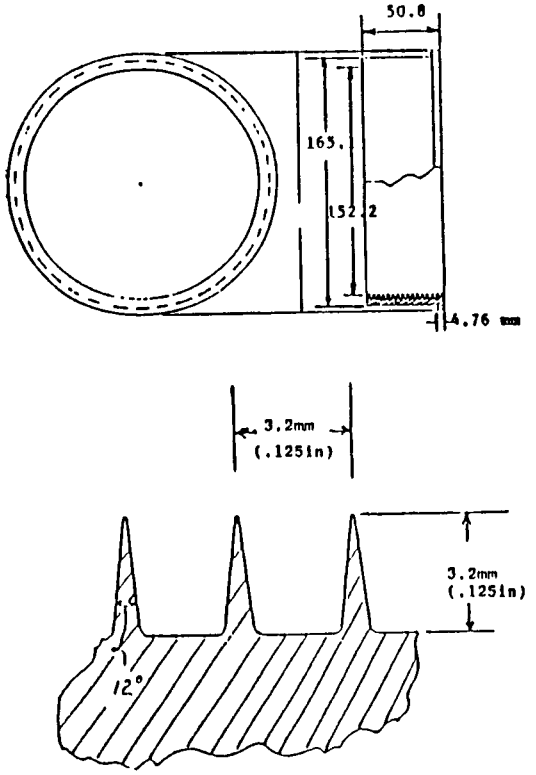

Figure 15. Labyrinth seal geometry.

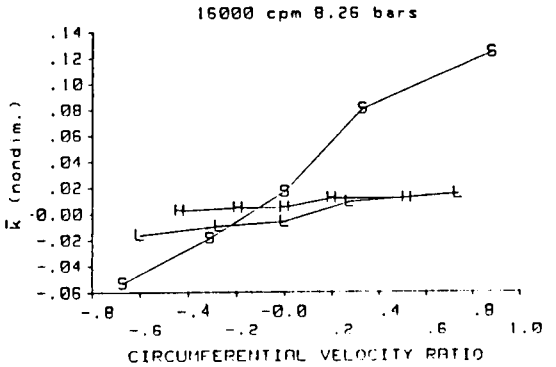

Figure 16. $\overline{k}$ versus $u_{\theta o}$ for smooth, labyrinth, and honeycomb seals.

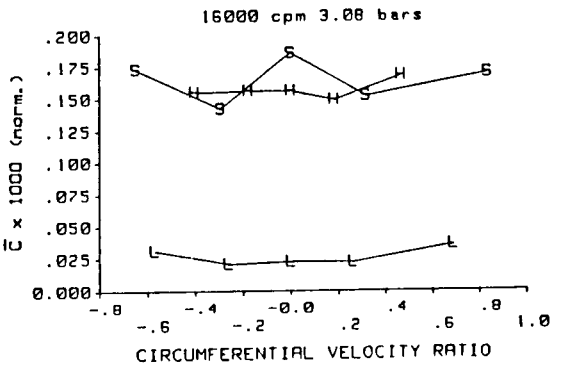

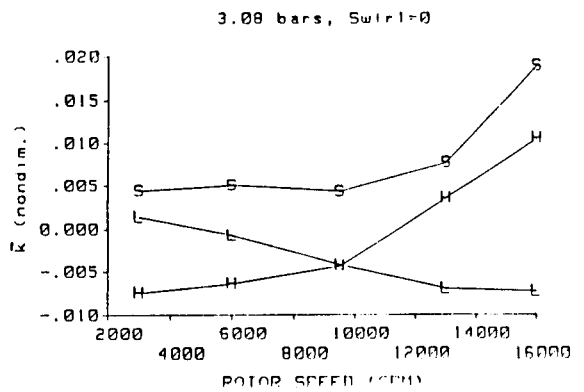

Figure 17. $\overline{k}$ versus ω for smooth, labyrinth, and honeycomb seals.

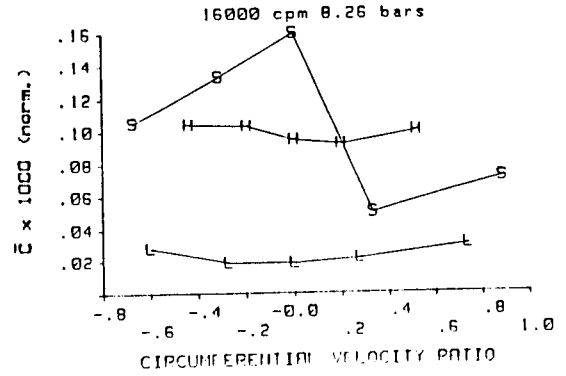

Figure 18. $\overline{C}$ versus $u_{\theta o}$ for smooth, labyrinth, and honeycomb seals.

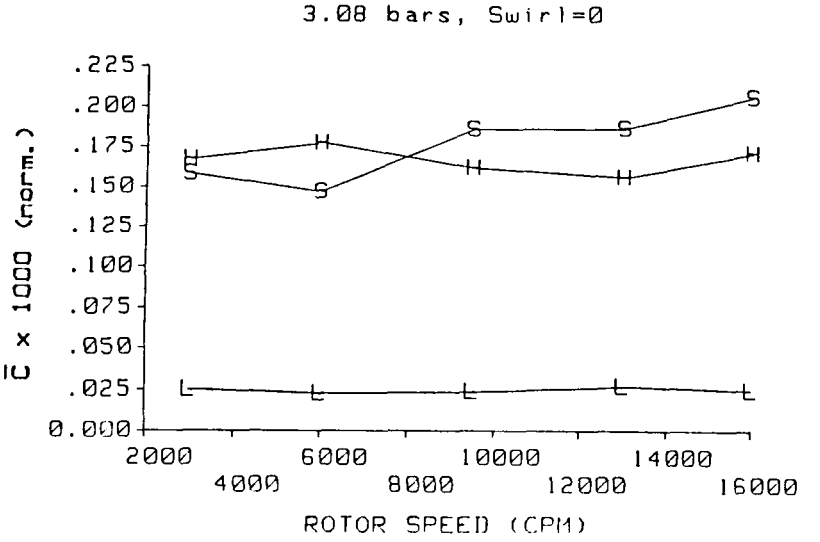

Figure 19. $\overline{C}$ versus ω for smooth, labyrinth, and honeycomb seals.

Whirl Frequency Ratio Results

Figure 20 shows f versus $u_{\theta o}$ for the smooth, labyrinth, and honeycomb seals. For negative $u_{\theta o}$, the labyrinth seal is the most stable, and the honeycomb seal is the least stable. For $u_{\theta o} = 0$, the labyrinth seal is the most stable, and the smooth seal is the least stable. For positive $u_{\theta o}$, the honeycomb seal is the most stable, and the smooth seal is the least stable. A comparison of figures 20 and 12 reveals that the least stable honeycomb seal tested (seal 1 of table 1) is more stable than the smooth and labyrinth seals for positive $u_{\theta o}$.

Direct Stiffness Results

Figure 21 illustrates $\overline{K}$ versus $u_{\theta o}$ for a rotor speed of 16000 cpm, and an inlet pressure of 8.26 bars. For the honeycomb seal, $\overline{K}$ is positive and relatively insensitive to changes in $u_{\theta o}$. For the labyrinth seal, $\overline{K}$ is negative and independent of $u_{\theta o}$. For the smooth seal, $\overline{K}$ is negative for no prerotation of the inlet air and increasingly positive for increasing, positive $u_{\theta o}$. Recall from figures 13 and 14 that honeycomb-cell-dimension differences yield markedly different direct stiffness values. Fortunately, the K values for annular gas seals tend to have a second-order influence on rotor response and stability.

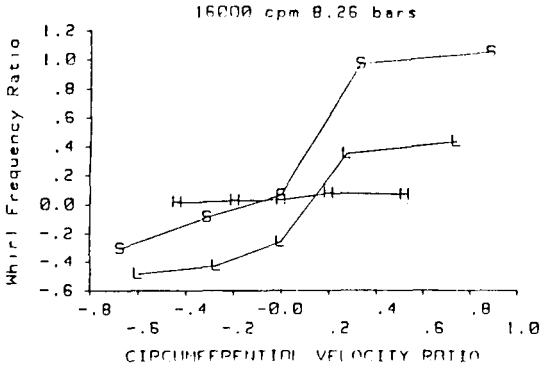

Figure 20. Whirl frequency ratio versus $u_{\theta o}$ for smooth, labyrinth, and honeycomb seals.

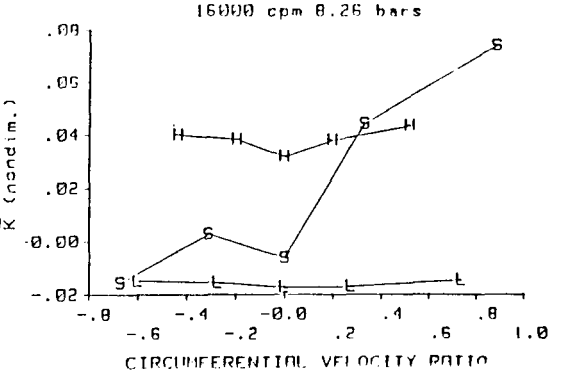

Figure 21. $\overline{K}$ versus $u_{\theta o}$ for smooth, labyrinth, and honeycomb seals.

LEAKAGE PERFORMANCE

Honeycomb Seal Results

Figure 22 illustrate the flow coefficient,

$$\Phi = \frac{\dot{m}\sqrt{R_c T_r}}{\pi D C r P_r}, \tag{4}$$

for the seven honeycomb seals in table 1. All seven seals are unchoked at an inlet pressure of 3.08 bars, and choked at 8.26 bars. Φ is relatively insensitive to changes in the supply pressure. By comparison to figure 8, note the absence of correlation between leakage performance and $\overline{k}$. Changes in effective stator roughness which increase or decrease leakage do not yield corresponding changes in $\overline{k}$.

Relative Performance for Honeycomb, Labyrinth, and Smooth Stators

Figure 23 illustrates Φ versus $u_{\theta o}$ for the smooth, labyrinth, and honeycomb (seal 7 of table 1) stators. These are the same seals for which rotordynamic characteristics were compared in the preceding section. The results of figure 23 show that the honeycomb seal leaks the least, followed in order by the labyrinth and smooth seals. Although not illustrated, the results are insensitive to changes in running speed and supply pressure. By comparison to figure 22, note that all of the honeycomb seals leak less than the labyrinth.

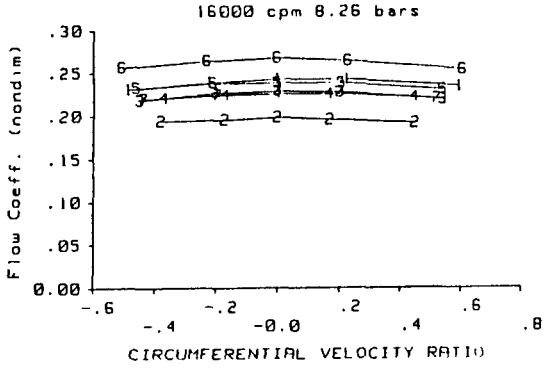

Figure 22. Flow coefficient versus $u_{\theta o}$ at 8.26 bars for the honeycomb seals of table 1.

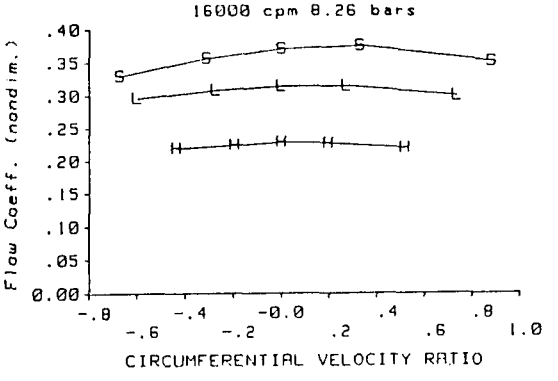

Figure 23. Flow coefficient versus $u_{\theta o}$ for the smooth, labyrinth, and honeycomb seals.

Discussion and Conclusions

The test results presented here show that honeycomb seals are sensitive to changes in cell dimensions; however, no clear patterns emerged for the seven seal configurations tested. Test results are needed for additional (deeper) cell depths to try to establish patterns of changes in rotordynamic coefficients and leakage due to changes in cell dimensions. Honeycomb seals are "damper" seals in the sense of von Pragenau (1982) in that the rough stator reduces the tangential velocity. By comparison between honeycomb and smooth seals, their effectiveness in reducing k (and presumably the tangential velocity) is clearly demonstrated. However, there is no correlation between leakage performance (effective roughness) and cross coupled stiffness magnitudes. Seals 2 and 6 are, respectively, the

best and worst leakage performers of figure 22; however, k for seal 6 is equal to or less than k for seal 2 in figure 9. Clearly, some physical factor other than surface roughness must be accounted for to explain the effectiveness of honeycomb stators in reducing k.

The frequency dependency of the honeycomb-seal rotordynamic coefficients may be explained, in part, by Tam et al.'s paper (1987). Their numerical solutions show that "small" motion of a rotor which is sufficient to excite measureable dynamic forces, may create secondary flow and disturb the "base" flow solution. The cell depths are much too short to yield Helmholtz resonances of the gas within the honeycomb seal cavities within the frequency range of interest. The fact that frequency-independent coefficients are obtained for other seal configurations would seem to eliminate the dynamic response of the test rig as a source of the observed frequency dependency. Future tests are planned for honeycomb seals using a swept-sine-wave excitation which may provide additional physical insight of the observed frequency dependence.

Leakage comparisons, at the same minimum clearances, demonstrate the superiority of honeycomb stators followed in order by labyrinth and smooth stators. Rotordynamic measurements show that the direct damping of honeycomb and smooth stators are greater by a factor of approximately six than labyrinth stators. Obviously, increased damping means reduced rotor response when operating near or through critical speeds. With respect to rotordynamic stability, the honeycomb stators are best if the flow entering the seal is prerotated in the direction of rotation. However if the fluid is not prerotated, the labyrinth seal is better. In practical terms, the honeycomb seal is better, in the absence of an effective swirl brake, and the labyrinth seal is better if used with an effective swirl brake. There is no reason to use a swirl brake with a honeycomb seal.

As noted at the beginning of this section, the characteristics of honeycomb seals are sensitive to changes in cell dimensions; hence, the present test results should be viewed as preliminary. Additional tests are required at deeper cell depths and additional clearances.

REFERENCES

Benckert, H, and Wachter, J., (1980), "Flow Induced Spring coefficients of Labyrinth Seals for Applications in Rotordynamics," proceedings of a workshop held at Texas A&M University, 12-14 May 1980, NASA CP2133, *Rotordynamic Instability Problems in High Performance Turbomachinery,* pp. 189-212.

Childs, D. W., Elrod, D. A., Hale, R. K., (1986), "Rotordynamic Coefficient and Leakage Test Results for Interlock and Tooth-on-Stator Labyrinth Seals," accepted for presentation at the ASME International Gas Turbine Conference, May 1988.

Childs, D., and Kim, C-H, (1985) "Analysis and Testing for Rotordynamic Coefficients of Turbulent Annular Seals with Different Directionally Homogeneous Surface Roughness Treatment for Rotor and Stator Elements," *ASME Transaction Journal of Tribology Technology,* Vol. 107, July 1985, pp. 296-306.

Childs, D. W., Nelson, C. C., Nicks, C., Scharrer, J., Elrod, D., Hale, K., (1987), "Theory Versus Experiment for the Rotordynamic Coefficients of Annular Gas Seals: Part 1, Test Facility and Apparatus," *ASME Trans. J. of Tribology,* Vol. 108, pp. 426–432.

Childs, D. W. and Scharrer, J. K., (1987), "Theory Versus Experiment for the Rotordyanmic Coefficients of Labyrinth Gas Seals: Part II - A Comparison to Experiment," *ASME Rotating Machinery Dynamics*, Vol. 1, pp. 427-434.

Cohen, H., Rogers, C. F. G., and Saravanamutto, H. H., (1972), *Gas Turbine Theory*, Longman Group Limited.

Hisa, S., Sahakida, H., Asata, S., and Sakamoto, T., (1986) "Steam Excited Vibration in Rotor-bearing System, proceedings of the IFToMM International Conference, Tokyo, Japan, 14-17 September 1986, pp. 635-641.

Holman, J. P., (1978), *Experimental Methods for Engineers*, McGraw-Hill, New York, NY, pp. 45.

Tam, L. T., Przekwas, A. J., Muszynska, A., Hendricks, R. C., Braun, M. J., and Mullen, R. L., (1987), "Numerical and Analytical Study of Fluid Dynamic Forces in Seals and Bearings," *ASME Rotating Machinery Dynamics*, Vol. 1, pp. 359-370.

von Pragenau, G. L., (1982), "Damping Seals for Turbomachinery," NASA Technical Paper 1987.